

**Course Notes: Topics in Computational  
Structural Biology.**

**Bruce R. Donald**

**June, 2010**

**Copyright © 2012**

# Contents

<b>11 Computational Protein Design</b>	<b>1</b>
11.1 Introduction . . . . .	1
11.2 Overview of Methodology . . . . .	2
11.3 Algorithm Design . . . . .	2
11.4 Intuition: Dead-End elimination . . . . .	6
11.5 Complexity Analysis . . . . .	8
11.6 Experimental Validation: Interplay of Computational Protein Design and NMR . . .	9

# Chapter 11

## Computational Protein Design

*This is an example Chapter for our course notes. It is taken from Chapter 11 of the Textbook. A PDF of this chapter is freely available at the MIT Press Web site.*

This lecture introduces the automated protein design and experimental validation of a novel sequence, as described in [1].

### 11.1 Introduction

Given a 3-D backbone structure, the *protein design* problem is to find an optimal sequence that satisfies the physical chemical potential functions and stereochemical constraints. Protein design is an “*inverse folding problem*”, and fundamental for understanding the protein function.

The term *rotamer* denotes discrete rotational conformations of protein sidechains. Typically these are represented by a finite discretization of the sidechain  $\chi_1, \chi_2, \dots$  dihedral angles. Rotamers are based on observed sidechain conformations from a statistical analysis of high-resolution crystal structures in the PDB. A rotamer can encode a different conformation of the same amino acid sidechain, or a switch in amino acid type. Both are encoded uniformly

using a rotamer *library* that contains the low-energy sidechain conformations across different amino acids.

The most basic protein design problem is often viewed as a search for the optimal rotamers to fit on a given protein backbone. Typically, the  $C^\alpha$ - $C^\beta$  bond remains invariant unless the residue is mutated to glycine or proline. The search returning the optimal rotamers yields both sidechain conformations and underlying design sequence. The sequence of the computed rotamers can be obtained by examining the amino acid type of each residue while disregarding its sidechain conformation. However, structural confirmation of a designed structure requires comparing the predicted side-chains (and backbone) versus the experimentally-determined structure by x-ray crystallography or NMR.

## 11.2 Overview of Methodology

*The following is the methodology used in [1]:*

Given a backbone fold of a target structure, [1] first developed an automated side-chain selection algorithm to (1) screen all possible amino acid sequences, and (2) find the optimal sequence and side-chain orientations (rotamers). Then experimental validation by using NMR was performed to evaluate the computed optimal sequence/structures.

## 11.3 Algorithm Design

**Input:** Backbone fold (Zif268), represented by structure coordinates.

**Output:** Optimal sequence (FSD-1)

**Overview:**

- (1) The algorithm considers specific interactions between (a) side-chain and backbone and (b) side chain and side chain.
- (2) The algorithm scores a sequence arrangement, based on a van der Waals potential function, solvation, hydrogen bonding, and secondary structure propensity [1].
- (3) The algorithm considers a discrete set of rotamers, which are all allowed conformers of each side chain.
- (4) The algorithm applies a *dead-end elimination* (DEE) algorithm to prune rotamers that are inconsistent with the global minimum energy solution of the system.

**Details:**

The inputs of the algorithm are structure coordinates of the target motif's backbone, such as N, C<sub>α</sub>, C' and O atoms, and C<sub>α</sub>-C<sub>β</sub> vectors. The residue positions in the protein structure are partitioned into *core*, *surface*, and *boundary* classes. The set of possible amino acids at the core positions is {Ala, Val, leu, Ile, Phe, Tyr, Trp}. The set of amino acids considered at the surface positions is {Ala, Ser, Thr, His, Asp, Asn, Glu, Gln, Lys, Arg}. The combined set of both core and surface amino acids are considered for the boundary positions.

**Note:** The total number of possible amino acid sequences is equal to the product of possible amino acids at each residue position. For instance, suppose that there are 7 possible amino acids at one core position, and 16 possible amino acids at each of 7 boundary positions, and 10 possible amino acids at each of 18 surface positions. The search space consists of  $7 \times 16^7 \times 10^{18} = 1.88 \times 10^{27}$  possible amino acid sequences.

The algorithm is divided into two phases:

**Phase 1 (Pruning):** The algorithm applies DEE to find and eliminate rotamers that are dead-ending with respect to the global minimum energy solution (GMEC). A rotamer  $r$  at the residue position  $i$  will be eliminated (i.e., proven to be dead-ending) if there is another rotamer  $t$  at the same position such that replacing  $r$  by  $t$  will always reduce the energy. However, naïvely checking this will still take exponential time. Therefore the following pruning was applied. Below,  $i_r$  denotes rotamer  $r$  at sequence position  $i$ . Similarly,  $i_t$  and  $j_s$  denote, respectively, rotamer  $t$  at position  $i$ , and rotamer  $s$  at position  $j$ .

**DEE Condition:** If there exists a rotamer  $t$  satisfying

$$E(i_r) - E(i_t) + \sum_j \min_s (E(i_r, j_s) - E(i_t, j_s)) > 0, \quad (11.1)$$

then  $r$  will be eliminated, where  $E(i_r)$  and  $E(i_t)$  represent *self-energies*, i.e., energies between the atoms of a single rotamer (e.g.,  $i_r$ ). By convention, and for convenience, we include in the self-energy term the *rotamer-template energies* also. In this context, ‘template’ means the geometric structure of the protein backbone atoms.  $E(i_r, j_s)$  and  $E(i_t, j_s)$  represent residue *pairwise*, rotamer-rotamer energies for rotamers  $i_r$ ,  $i_t$ , and  $j_s$ . The condition in Eq. (11.1) ensures that replacing  $r$  by  $t$  will always reduce the energy, regardless of what the rotamers at other residue positions are. The intuition behind Eq. (11.1) is given in Sec. 11.4.

Note that we have ‘overloaded’ the operator  $E$  to represent both self-energies (e.g.,  $E(i_r)$ ) and residue-pairwise energies (e.g.,  $E(i_r, j_s)$ ). Many protein design algorithms (including most of those in this book) explicitly require that the energy function  $E$  be residue-pairwise additive. The DEE algorithms directly exploit this assumption. In general, DEE algorithms could, in principle, be extended to work with residue- $k$ -wise additive energy functions instead,

for a small constant  $k > 2$ . However, parameterizing such energy functions requires care, and can be difficult. In general, “ $N$ -body” energy functions (where  $N$  is the total number of atoms) such as the Generalized Born/Poisson-Boltzmann solvation models are not amenable to DEE. However, there are approximate pairwise solvation models, and these are discussed in Chapter 12.

Different scoring functions  $E$  are defined for core, surface and boundary residues separately. The scoring function for core residues uses “a van der Waals potential to account for steric constraints and an atomic solvation potential favoring the burial and penalizing the exposure of nonpolar surface area” [1]. The surface residues apply a hydrogen-bond potential and secondary structure propensities, and a van der Waals potential. The residues at the boundary positions use a combination of both core and surface scoring functions.

**Phase 2 (Enumeration):** For any residue position  $i$ , let  $R_i$  be the remaining rotamers that are not eliminated in the **Phase 1**. The algorithm then enumerates all the combinations of remaining rotamers—that is,  $\prod_i R_i$ —to find the combination that has the global minimal energy. Enhancements to DEE (e.g., [3, 2]) also prune *pairs* of rotamers that are inconsistent with the GMEC, returning only subsets  $R_{ij} \subset R_i \times R_j$  of the pairwise cross products. Rotamer pairs in  $R_i \times R_j$  but outside  $R_{ij}$  cannot participate in the GMEC.

Phase 1 is provably correct, in that no rotamer will be pruned if it is part of the GMEC. Phase 1 is also polynomial-time. Phase 2 can be made provable using the  $A^*$  search algorithm (Chapter 12 and [4]). That is,  $A^*$  after DEE will guarantee to compute the GMEC. Phase 2 is worst-case exponential-time.

### Results:

Figure 11.1 shows the comparison of optimal computed sequence FSD-1 and the target

sequence Zif268. Figure 11.2 shows the comparison of the experimentally-determined structure of the optimal computed sequence FSD-1, versus the structure of the target backbone sequence Zif268.

## 11.4 Intuition: Dead-End elimination

Here is the intuition behind Equation (11.1), the Dead-End Elimination (DEE) condition. We repeat it here for clarity:

$$E(i_r) - E(i_t) + \sum_j \min_s (E(i_r, j_s) - E(i_t, j_s)) > 0. \quad (11.1)$$

Recall that lower energy is better; we are searching for the GMEC. The DEE condition (Equation 11.1) tells us that we can prune a *candidate* rotamer  $i_r$  if certain conditions hold. Those conditions include: the existence of a *competitor* rotamer  $i_t$  (i.e., a competitor rotamer  $t$ , also at position  $i$ ) that is better than  $i_r$ . But how can we prove that  $t$  is better than  $r$ ? For this calculation, it will be helpful to use the perspective of a *witness* rotamer  $j_s$ . In this biophysical modeling problem the only ‘perspective’ a witness can have on the discrete choice  $i_r$  vs.  $i_t$  is its energetic interaction with the candidate vs. the competitor. One of these energies will be more favorable, which implies we may construct a penalty for the choice of rotamer  $r$  vs.  $t$  at position  $i$ .

First, the DEE condition contains a local sidechain-backbone penalty encoding the cost of choosing  $i_r$  vs.  $i_t$ . This is  $E(i_r) - E(i_t)$ . It is independent of  $j_s$ .

The DEE condition also includes a pairwise sidechain-sidechain penalty for the cost of choosing  $i_r$  vs.  $i_t$ , from the perspective of  $j_s$ . Now, if we *knew* what rotamer  $s$  was at position  $j$ , then this penalty would simply be  $E(i_r, j_s) - E(i_t, j_s)$ . Since we don’t, all possible rotamers at position  $j$  must be considered. The pairwise penalty is built by computing at position  $j$





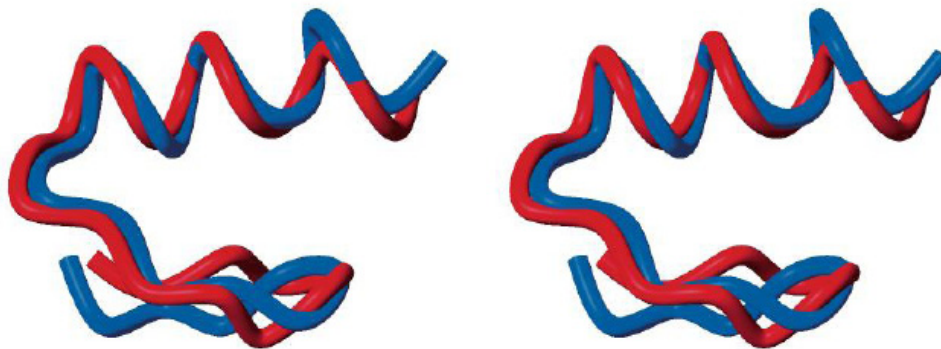


**Figure 11.2:** Backbone structure comparisons of computed sequence FSD-1 and the target sequence Zif268 [1]. Comparison of the FSD-1 structure (blue) and the design target (red). Stereoview of the best-fit superposition of the restrained energy minimized average NMR structure of FSD-1 and the backbone of Zif268. Residues 3 to 26 are shown. Credit: Ref. [1].

a *lower bound* on the  $i_r$  vs.  $i_t$  penalty, namely  $\min_s (E(i_r, j_s) - E(i_t, j_s))$ . The minimization occurs over all *possible* rotamers  $s$  at position  $j$ . Then a sum is computed of *all* such lower bounds over all residue positions:  $\sum_j \min_s (E(i_r, j_s) - E(i_t, j_s))$ . If the entire quantity on the left-hand side in equation Eq. (11.1) is positive, then rotamer  $i_r$  can be pruned, since we have proven it cannot participate in the GMEC.

Finally, the DEE criterion can be efficiently computed, in polynomial time, by enumerating triples of the form  $(i_r, i_t, j_s)$ . We prove this below.

## 11.5 Complexity Analysis

Let  $n$  denote the number of residues, and  $r$  denote the (maximum) number of possible rotamers for each residue.

We first analyze the time complexity of DEE pruning in Phase 1. For each rotamer at a specific residue position  $i$ , it takes time  $O(nr)$  to search all  $r$  possible amino acids in all other  $n - 1$  positions to find  $\sum_j \min_s [E(i_r, j_s) - E(i_t, j_s)]$ . Comparisons with other rotamers at the same position  $i$  take  $r \cdot O(nr) = O(nr^2)$  time. Since we need to consider all possible

rotamers at every position  $i$ , the total DEE pruning takes  $n \cdot r \cdot O(nr^2) = O(n^2r^3)$  time. So DEE is polynomial time!

Although the pruning step will eliminate many states (that is, a configuration of rotamers) in the search space, it cannot guarantee that the number of the remaining states is small enough for the enumeration to be efficient. Even if there are only two rotamers remaining for each position, the worst-case time to find the state that minimizes energy is still exponentially large.

**Note:** In fact, the optimization problem in protein design has been proven NP-hard [5], and even NP-hard to approximate [6].

## 11.6 Experimental Validation: Interplay of Computational Protein Design and NMR

The solution structure for the computed sequence FSD-1 was obtained by using 2D  $^1\text{H}$  NMR spectroscopy. Sample NMR data, including a NOESY spectrum, are shown in Figure 11.3. X-PLOR plus the standard protocols for hybrid distance geometry-simulated annealing were used to calculate the structure. Figure 11.4 and 11.5 show an ensemble of 41 structures that are consistent with good geometry and distance constraints within a small tolerance. The structure of FSD-1 was close to the target structure (Zif268), validating the structure-based protein design algorithm using DEE.

The structure determination in [1] also represents a simple didactic example of the classic method of NMR protein structure determination in the solution state, based primarily on NOEs. Although FSD-1 is a small protein, the basic concepts such as sequential and short range NOEs, NOESY crosspeaks, NOESY assignment, structural ensembles, and the



**Table 1.** NMR structure determination: distance restraints, structural statistics, and atomic root-mean-square (rms) deviations.  $\langle SA \rangle$  are the 41 simulated annealing structures,  $SA$  is the average structure before energy minimization,  $\langle SA \rangle_r$  is the restrained energy minimized average structure, and SD is the standard deviation.

Distance restraints		
Intraresidue		97
Sequential		83
Short range ( $ i - j  = 2$ to 5 residues)		59
Long range ( $ i - j  > 5$ residues)		35
Hydrogen bond		10
Total		284
Structural statistics		
rms deviations	$\langle SA \rangle \pm SD$	$\langle SA \rangle_r$
Distance restraints (Å)	$0.043 \pm 0.003$	0.038
Idealized geometry		
Bonds (Å)	$0.0041 \pm 0.0002$	0.0037
Angles (degrees)	$0.67 \pm 0.02$	0.65
Impropers (degrees)	$0.53 \pm 0.05$	0.51
Atomic rms deviations (Å)*		
	$\langle SA \rangle$ versus $SA \pm SD$	$\langle SA \rangle$ versus $\langle SA \rangle_r \pm SD$
Backbone	$0.54 \pm 0.15$	$0.69 \pm 0.16$
Backbone + nonpolar side chains†	$0.99 \pm 0.17$	$1.16 \pm 0.18$
Heavy atoms	$1.43 \pm 0.20$	$1.90 \pm 0.29$

\*Atomic rms deviations are for residues 3 to 26, inclusive. Residues 1, 2, 27, and 28 were disordered [ $\phi$ ,  $\psi$ , angular order parameters ( $34$ )  $< 0.78$ ] and had only sequential and  $|i - j| = 2$  NOEs. †Nonpolar side chains are from residues Tyr<sup>3</sup>, Ala<sup>5</sup>, Ile<sup>7</sup>, Phe<sup>12</sup>, Leu<sup>19</sup>, Phe<sup>21</sup>, Ile<sup>22</sup>, and Phe<sup>25</sup>, which constitute the core of the protein.

**Figure 11.4:** NMR structure determination of FSD-1. Credit: Ref. [1].

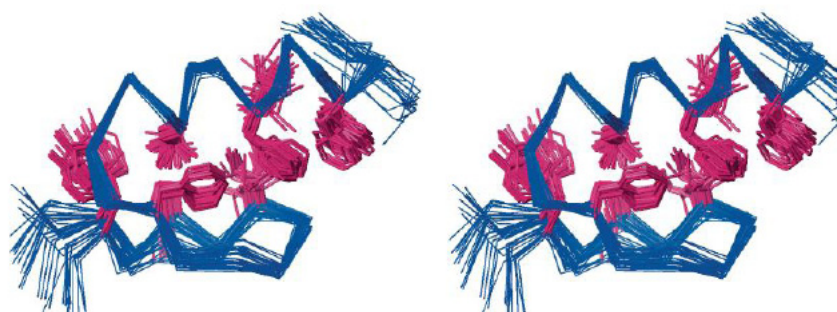


**Fig. 5.** Solution structure of FSD-1. Stereoview showing the best-fit superposition of the 41 converged simulated annealing structures from X-PLOR (37). The backbone  $C_{\alpha}$  trace is shown in blue and the side-chain heavy atoms of the hydrophobic residues (Tyr<sup>3</sup>, Ala<sup>5</sup>, Ile<sup>7</sup>, Phe<sup>12</sup>, Leu<sup>19</sup>, Phe<sup>21</sup>, Ile<sup>22</sup>, and Phe<sup>25</sup>) are shown in magenta. The amino terminus is at the lower left of the figure and the carboxyl terminus is at the upper right of the figure. The structure consists of two antiparallel strands from positions 3 to 6 (back strand) and 9 to 12 (front strand), with a hairpin turn at residues 7 and 8, followed by a helix from positions 15 to 26. The termini, residues 1, 2, 27, and 28 have very few NOE restraints and are disordered.

**Figure 11.5:** Empirically-determined NMR structure ensemble of FSD-1, including side-chains. Credit: Ref. [1].

# References

- [1] B. I. Dahiyat and S. L. Mayo. De Novo Protein Design: Fully Automated Sequence Selection *Science*, October 3; 278 (5335):82, 1997.
- [2] Desmet J, De Maeyer M, Lasters I. Theoretical and algorithmical optimization of the dead-end elimination theorem. *Pac Symp Biocomput.* 1997:122-33. PubMed PMID: 9390285.
- [3] Lasters I, De Maeyer M, Desmet J. Enhanced dead-end elimination in the search for the global minimum energy conformation of a collection of protein side chains. *Protein Eng.* 1995 Aug;8(8):815-22.
- [4] A. Leach and A. Lemon. Exploring the conformational space of protein side chains using dead-end elimination and the  $A^*$  algorithm. *Proteins*, 33:227–239, 1998.
- [5] Niles Pierce and Erik Winfree. Protein Design is NP-Hard. *Protein Engineering*, v15, pp. 779-782, 2002.
- [6] Bernard Chazelle, Carl Kingsford, Mona Singh. A Semidefinite Programming Approach to Side Chain Positioning with New Rounding Strategies. *INFORMS Journal on Computing*, 16(4): 380-392 (2004).